Draft version May 11, 2020
Typeset using LaTeX **twocolumn** style in AASTeX62

Ammonia Measurements in W51

Josh Machado,[1] Cara Battersby,[1] and Adam Ginsburg[2]

[1] *University of Connecticut*
Department of Physics
2152 Hillside Road, Unit 3046
Storrs, CT 06269-3046, USA
[2] *University of Florida*
Department of Astronomy
Bryant Space Science Center
Stadium Road
Gainesville, FL 32611, USA

ABSTRACT

We found things! The abstract should include a summary of the overarching questions motivating the work, the methods you used, and the results you found. AA uses the model of "Context, Aims, Methods, Results." This can be the last thing you write if you want.

1. INTRODUCTION

(XX this is a comment) comment

Massive stars are among the most important drivers of change in our universe. They provide the UV light necessary to ionize galaxies and create the heavy elements required for life. Yet despite their importance, the process by which the most massive stars form is not well understood.

Being among the most massive and active star forming regions in the Milky Way, W51 (see Fig. 1) is excellent laboratory for studying star formation [reference]. W51 is a giant molecular cloud complex at a distance of 5kpc (add exact best estimate here, along with reference for it). This region has been studied extensively in existing literature. This project uses observed ammonia emission within W51 to study the region's physical properties, and the masses of protostellar cores embedded within it. Due to its molecular structure, ammonia's inversion transitions provide a very accurate probe of temperature [reference here?]. Observing NH_3 emission also provides measurements of other physical parameters such as line widths, velocities and ammonia column densities. This study aims to obtain more detailed mass and temperature measurements for a catalog of previously identified cores in the region [reference to Adam's W51 ALMA paper]. We also look to see how these measurements relate to the current understanding of the core mass function (CMF).

Observations and data are described in Section 2 .Data analysis, ammonia fitting and methodology are described in Section 3. The results are presented in Section 4 and discussed in Section 5. Conclusions and further work are discussed in Section 6.

2. DATA

2.1. *VLA Observations*

Observations were made with the National Radio Astronomy Observatory's Karl G. Jansky Very Large Array on January 1, 2016. Two primary regions within the W51 cloud complex were observed, W51 Main (19:23:45.0, +14:30:11.0) and IRS2 (19:23:40.0, +14:30:35.0). K-band observations, lasting 6 hours, captured the (1,1), (2,2), (3,3), (4,4), and (5,5) ammonia inversion transitions, as well a 22GHz water maser.

The observations consisted of two separate pointings, one covering W51 Main, the other, IRS2. Prior to any cleaning or imaging, the observations were reduced using version 5.1.2-4 r40000 of the VLA CASA Calibration Pipeline. The two fields were cleaned separately using CASA's `tclean` task after continuum subtraction via `uvcontsub`. With the exception of the W51 Main (4,4) and (5,5) spectral windows, all fields were cleaned using automasking. W51 Main field was cleaned with custom made masks, while the IRS2 field was cleaned with automasking. Once cleaned separately, the two fields were linearly mosaiced with CASA's `linmos` task. All analysis was done with the full field data cubes produced by `linmos`. Scripts for `uvcontsub`, `tclean` and `linmos` can be found on Github.

2.2. *Supplemental ALMA Data*

ALMA observations of W51 presented in Ginsburg et al. 2017 (reference) were used in combination with

Table 1. W51 Observational Parameters

Parameter	NH_3 (1,1)	NH_3 (2,2)	NH_3 (3,3)	NH_3 (4,4)	NH_3 (5,5)
Rest Frequency	23.69447 GHz	23.72260 GHz	23.87008 GHz	24.13935 GHz	24.53292 GHz
BMAJ	5.036"	4.039"	4.716"	5.613"	4.299
BMIN	3.149"	3.172"	3.206"	3.187"	3.136
Channel Width	7.812 kHz	15.625 kHz	7.812 kHz	7.812 kHz	7.812 kHz
Spectral Resolution	0.1 km s^{-1}	0.2 km s^{-1}	0.1 km s^{-1}	0.1 km s^{-1}	0.1 km s^{-1}
RMS/channel	1.5 mJy	1.5 mJy	1.5 mJy	2 mJy	2 mJy

the VLA data. ALMA observed the region with a 37-pointing mosaic at 226GHz, achieving a resolution of 0.2".

3. METHODS

3.1. *Ammonia Fitting*

To create physical parameter maps of the region, the observed spectra were fit with an ammonia model. Using a python spectral fitting toolkit, `pyspeckit`, developed by Adam Ginsburg, each pixel of the reduced full field data cubes where fit. These fits were done using the (1,1), (2,2) and (4,4) inversion transitions of ammonia. Based on the ratio of pixel brightness to RMS, pixels with a low signal to noise ratio (SNR <3) were excluded from the fitting process. An error map generated from the (1,1) data cube was included in the fitting script to aid in calculating parameter uncertainties. The error map was a full field flat value of 1.5mJy. This value was determined by averaging the RMS in emission free channels of the (1,1) data cube. This same error map was applied to the (2,2) and (4,4) data cubes as well.

Several initial guesses and parameter restrictions were applied during the process to help the fitter converge on reasonable values. An intensity-weighted velocity map of the (1,1) data cube was inputted into the fitting process to provide line width estimates. Temperature estimates were confined to a range of 2.7315 to 150K for kinetic temperature, and 2.7315 to 30K for rotational temperature. The ortho-to-para ratio was fixed at 0.5 for all fits and centroid velocity was confined to a range of 40 to 75 km s^{-1}

Resulting fits provided estimates of kinetic temperature, rotational temperature, centroid velocity, line width and ammonia column density. The `pyspeckit` ammonia fitter also provides estimated uncertainties for each parameter value. For regions with no detected (4,4) emission the same fitting process described above was used, but instead `pyspeckit`'s cold ammonia model was used. All fits were limited by a single component emission model.

AG note: Need to describe regions where 4,4 was (not) used. Probably need to show that in a figure

3.2. *Core Mass Measurements & CMF Fitting*

The resulting ammonia fitted temperatures were used to measure the masses of a catalog of protostellar cores identified in Ginsburg et al. 2017. In combination with a 1mm ALMA continuum map of the region (Ginsburg et al. 2017), the ammonia derived temperatures were used to calculate a gas surface density. Gas and dust temperatures are assumed to be closely coupled. Therefore, ammonia derived temperatures are assumed to be equivalent to the gas temperatures. Surface density measurements were then calculated by the following relation:

$$\Sigma_{gas} = C(\nu)c^2(2kT_{NH3} * \kappa_{gas}\nu^2)^{-1}(\nu/\nu_0)^{-\beta}$$

where $C(\nu)$ is the intensity of ALMA 1mm continuum observations (Ginsburg et al. 2017), $\nu = 226$GHz, $\nu_0 = 271.1$GHz, $\kappa_{gas} = 0.0114\text{cm}^2\text{g}^{-1}$ and $\beta = 1.75$. A dust to gas ratio of 100 was assumed in this process. With the resulting surface densities, mass was determined via:

$$M/M_\odot = \Sigma_{gas} * area$$

where *area* is determined by beam area and current estimates of the distance IRS2 & W51 Main [citation]. This process of calculating protostellar core masses was completed using temperatures derived from `pyspeckit`'s base ammonia model and cold ammonia model.

Of the 77 cores originally identified in Ginsburg et al. 2017, 61 sources were detected in ammonia emission. Of the 61 sources detected in ammonia emission, only num went undetected in (4,4) emission and were fit with a cold ammonia model. Masses were compiled into two separate catalogs, one with and one without the cold ammonia fits. These catalogs were then compared to existing core mass measurements from Ginsburg et al. 2017. Using the python package `powerlaw` to fit a power law, a measurement of the CMF in the region was obtained. Measurements of the α value of the CMF powerlaw were then compared to existing works.

4. RESULTS

The `pyspeckit fiteach` task was largely successful in fitting the observed ammonia emission and achieving measurements of various physical parameters. However,

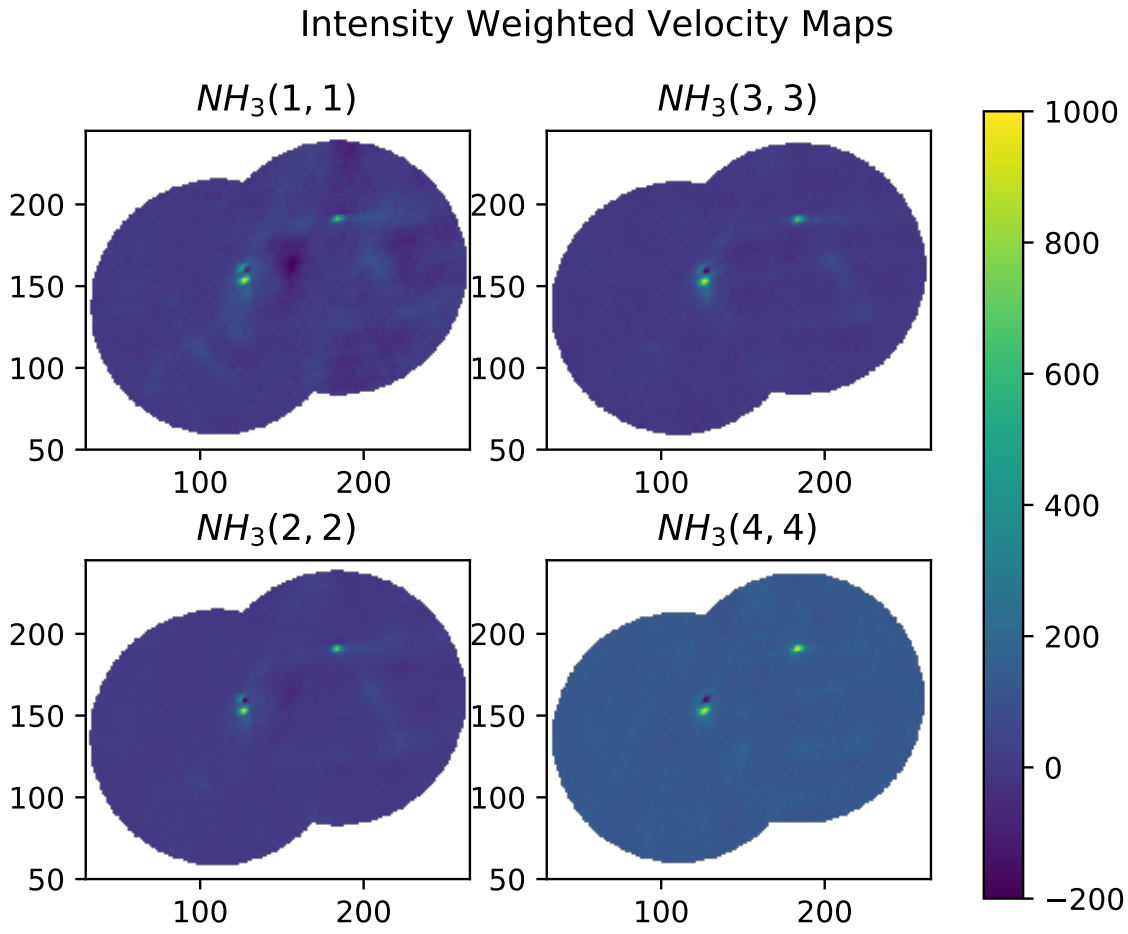

Figure 1. The moment zero maps for the (1,1) through (4,4) line emission are shown. The negative features seen in the (1,1) through (3,3) maps are a result of continuum absorption in the HII region within W51. The features only appear negative after continuum subtraction.

some regions proved to be problematic for fitting, due to complex emission and likely multi-component spectra. Failed fits are also apparent in the various parameter maps, most often found at the extremes of the parameter values. This will be resolved at a later time, potentially with more complicated fitting models.

The resulting fits from the `fiteach` task allowed for the creation of spacial parameter maps. Of particular importance is the ammonia derived kinetic temperatures. Shown in the top left panel of Fig. 2, the spatial kinetic temperature map displays a large variation in temperature. Most of the region exists in the 20-60 K range while the E2/E8 and IRS2 sub-regions exhibit higher temperatures (80K and above 120K respectively).

Greater column density and line widths also exist in regions of higher temperatures, as seen in Fig. 2.

Pyspeckit's ammonia fitting model produces a cube of parameter maps. From this, a map of kinetic temperature was obtained (see Fig 3). The field has a wide range of temperatures, peaking above 140K in IRS2. This is likely due to heating from massive young stars embedded in the region. Virtually all of the emission in the field is observed at temperatures greater than those typically seen in more nearby molecular clouds (Friesen et al. 2017). However, one feature south of IRS2 has temperatures around 20K, which is more inline with nearby molecular cloud temperatures.

The pyspeckit fitting process also produced a line width map for the region. W51 generally has much wider line widths when compared to local molecular clouds. In nearby molecular clouds, typical line widths are less than 1 km/s (Friesen et al. 2017), while the majority of the W51 Main & IRS2 region exceeds this typical value (see Fig 4). However, one region (shown in dark purple in Fig. 4) south of IRS2 contains narrow line widths analogous to those observed by Friessen (2017).

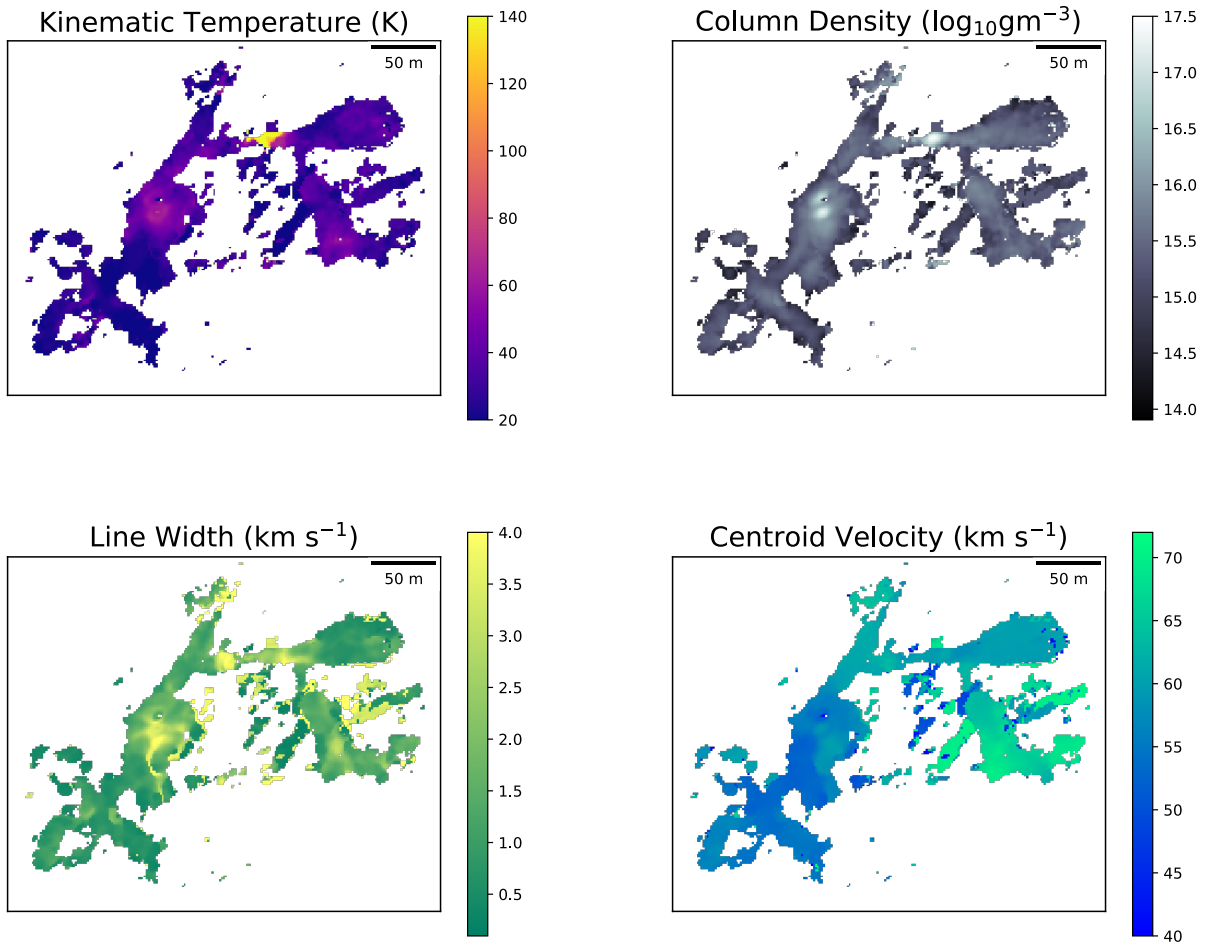

Figure 2. Various parameter maps of the observed field are shown. These are all derived from the fitting process described in Section 3 using `pyspeckit`'s base ammonia model.

It may be that this particular cloud is not yet interacting with the other nearby turbulent regions, but this still remains unclear. It is also worth noting that this narrow velocity feature has temperatures closer to typical nearby molecular cloud temperatures (around and below 20K). Since this particular cloud exhibits features similar to those seen in nearby molecular clouds, it will likely be a focus for further analysis.

Previously, a catalog of 76 cores were identified in the region (Ginsburg et al. 2017). Using the methods described above (Sec. 3), updated masses of previously identified cores were measured (see Table 1). However, of the 76 cores in the existing catalog, only 61 were detected in ammonia emission, and thus were able to have updated masses measured (see Fig 16 for core mass PDF). Comparing measurements to the existing catalog shows that these new ammonia temperature measurements constrain estimates of the core masses (see Fig. 5), suggesting that the 2017 catalog may have overestimated the core masses.

Having two separate mass measurement catalogs for the cores within W51 allowed for some analysis of the core mass function (CMF) in the region. Still a very active and open ended area of research, the CMF is a powerlaw function that describes the distribution of protostellar core masses. Not a lot is known about the CMF, but if properly characterized, it would prove to be a very useful tool in understanding star formation. An important question in regards to the CMF is whether or not it is universal. To help answer this, the CMF is often characterized in various environments to compare regions. Using the python package powerlaw, an estimate for the α value of the CMF was determined for both catalogs. It was found that $\alpha = 1.67 \pm 0.10$ for the updated ammonia catalog and $\alpha = 1.71 \pm 0.09$ for Ginsburg. These updated, ammonia constrained mass

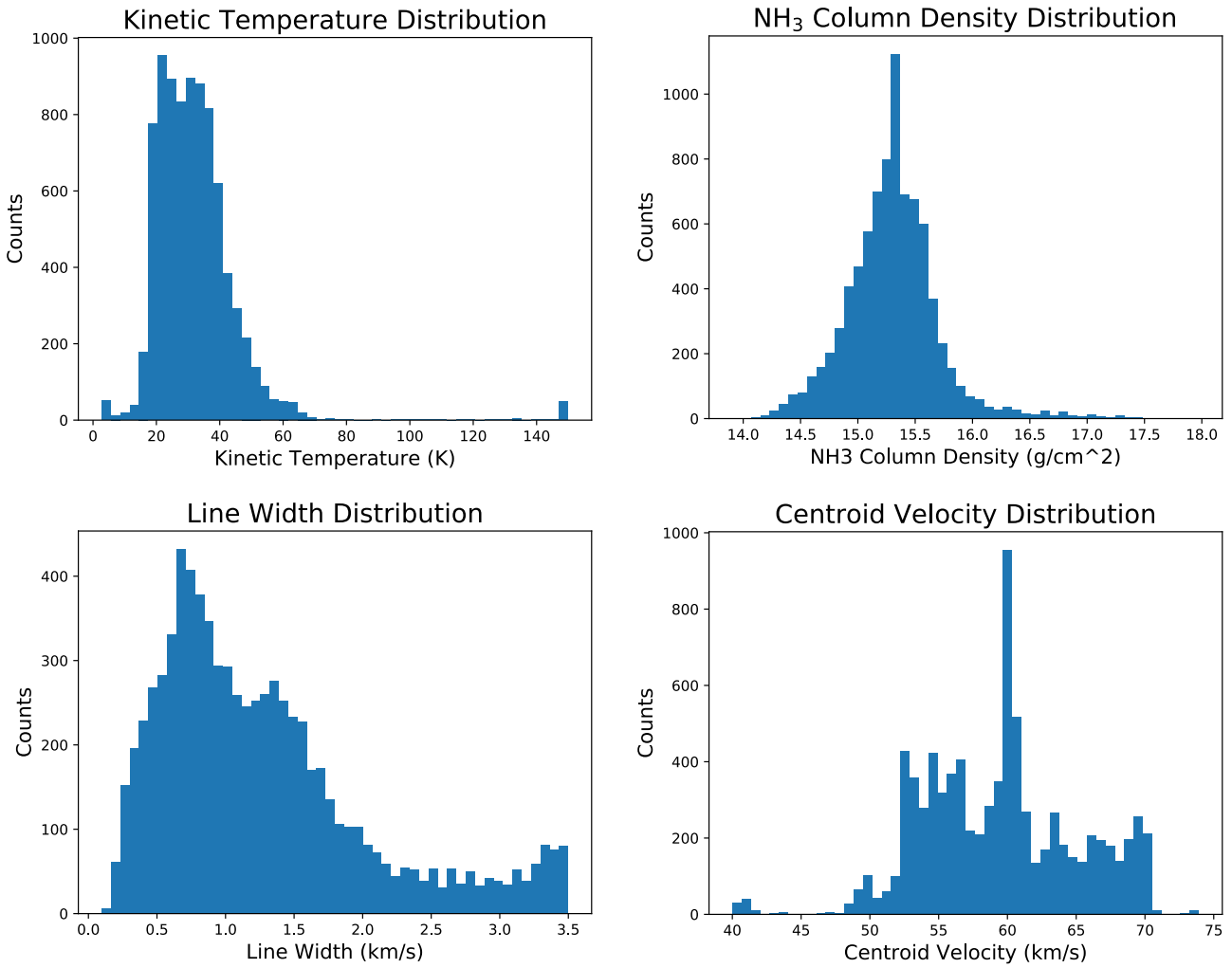

Figure 3. Distributions of parameter maps shown in Fig. 2. Line widths greater than 3.5 km s $^{-1}$ were excluded from the distribution as they are likely nonphysical and due to fitting limitations.

measurements did not alter the current estimate of the region's CMF in any statistically significant way.

To put these values of α in context with existing measurements in other environments, these data were compared to a similar study by Motte et al. 2016. Motte studied W43, a similar molecular cloud with 143 identified cores. Their group determined a value of $\alpha = 2.03 \pm 0.09$ for their cores. However, due to size-of-sample errors between the Motte catalog and our W51 catalog, no real statistical conclusions can be drawn in regards to the CMF.

5. DISCUSSION

Let's discuss.

5.1. *Limitations & Improvements for Fitting*

Discuss how fits are limited, uncertainties and improvements.

5.2. *Temperature & Kinematics of W51*

Discuss physical significance of temperature variation, velocity dispersion, etc.

5.3. *Core Mass Function*

Discussion of implications of CMF fitting and comparisons.

5.4. *Regions of Interest*

Narrow line width discussion and comparisons to nearby GMCs.

6. CONCLUSION

This project provided updated and more accurate estimations of the temperatures and core masses found within W51. A previously unidentified region of interest was identified through the temperature and line width maps. Additionally, this work helped to constrain the

core masses found in Ginsburg et al. 2017. From the measured core masses, an estimate of the CMF in the region was determined. However, due to sample size errors, no definitive conclusions can be drawn in regards to current estimates of alpha.

There is a lot of work left to be done for this project that will be tackled over the coming months. A few priorities are as follows: refit with the pysepckit cold ammonia model for regions that lack 4-4 detection, mask out bad fits or fit with a different method/more complex model, incorporate existing GBT NH_3 data into analysis, and of course further analyzing the narrow line width feature south of IRS2. This work will be continued with the help of Adam Ginsburg and my home institution advisor, Cara Battersby over the next academic year. Along with continued analysis, I plan to put together a paper with the updated work.

7. ACKNOWLEDGEMENTS

NRAO REU program, Cara, Adam

8. FIGURES & TABLES

Table 2. Catalog of kinetic temperatures and masses for cores.

name	RA	Dec	KTemp	Core Mass	Mass Uncertainty
	°	°	K	$M_\odot$	$M_\odot$
ContinuumFreeOutflowSource1	290.92	14.51	0.0	0	0
ALMAmm38	290.92	14.51	0.0	0	0
ALMAmm6	290.93	14.50	31.63	0.598	0.504
ALMAmm3	290.93	14.50	0.0	0	0
ALMAmm7	290.92	14.51	0.0	0	0
ALMAmm1	290.93	14.50	0.0	0	0
ALMAmm10	290.91	14.51	30.417	1.040	0.159
ALMAmm19	290.93	14.52	45.85	0.730	0.070
ALMAmm12	290.91	14.51	34.86	1.157	0.170
ALMAmm57	290.92	14.51	0.0	0	0
ALMAmm2	290.93	14.50	0.0	0	0
ALMAmm39	290.92	14.52	0.0	0	0
ALMAmm54	290.91	14.51	18.90	2.362	5.098
ALMAmm52	290.91	14.51	41.90	1.067	1.931
ALMAmm47	290.93	14.52	31.04	1.470	0.110
ALMAmm22	290.92	14.52	0.0	0	0
ALMAmm53	290.91	14.51	2.73	17.747	5.924
ALMAmm20	290.92	14.52	33.66	1.541	0.143
ALMAmm13	290.91	14.51	40.40	1.349	1.226
ALMAmm45	290.91	14.52	27.17	2.024	0.277
ALMAmm40	290.92	14.52	39.76	1.386	0.147
ALMAmm4	290.93	14.50	32.40	1.909	0.4209
ALMAmm27	290.93	14.52	37.48	1.736	0.090
ALMAmm56	290.93	14.51	36.23	1.820	0.092
ALMAmm55	290.93	14.51	40.76	1.640	0.084
ALMAmm44	290.91	14.52	34.88	2.008	2.360
ALMAmm48	290.93	14.52	33.73	2.203	0.094
ALMAmm30	290.93	14.52	37.65	2.00	0.082
ALMAmm15	290.91	14.51	37.9516	2.022	2.615
ALMAmm26	290.93	14.51	39.76	1.976	0.078
ALMAmm29	290.92	14.51	0.0	0	0
ALMAmm21	290.92	14.52	35.74	2.242	0.134
ALMAmm18	290.93	14.52	0.0	0	0
ALMAmm5	290.93	14.50	36.86	2.515	0.407
ALMAmm28	290.93	14.51	58.00	1.634	0.068
ALMAmm49	290.93	14.51	45.68	2.374	0.072
ALMAmm25	290.92	14.51	35.14	3.210	0.283
ALMAmm23	290.92	14.52	52.14	2.169	0.283
ALMAmm51	290.93	14.51	48.35	2.409	0.070
ALMAmm46	290.92	14.51	0.0	0	0
ALMAmm17	290.92	14.52	0.0	0	0
ALMAmm43	290.91	14.52	67.14	1.794	0.250
ALMAmm37	290.92	14.51	0.0	0	0

Table 2 continued from previous page

name	RA	Dec	KTemp	Core M
ALMAmm50	290.93	14.51	48.35	2.618
ALMAmm58	290.92	14.52	0.0	0
ALMAmm11	290.91	14.51	38.34	3.516
ALMAmm9	290.92	14.50	0.0	0
ALMAmm36	290.91	14.52	63.72	2.466
ALMAmm41	290.93	14.51	47.48	3.358
ALMAmm16	290.91	14.52	33.84	5.157
eSmm4	290.93	14.50	52.09	3.705
e2se	290.93	14.51	53.03	4.140
e5	290.92	14.52	33.44	6.589
eEmm2	290.93	14.51	63.73	3.592
eEmm1	290.93	14.51	64.92	3.610
e3mm1	290.93	14.51	62.20	4.753
eEmm3	290.93	14.51	62.32	4.858
eSmm6	290.93	14.50	47.13	6.796
eSmm2a	290.93	14.51	54.29	6.306
eSmm1	290.93	14.51	59.10	6.410
eSmm3	290.93	14.50	51.57	7.525
eSmm2	290.93	14.51	54.29	7.737
ALMAmm34	290.92	14.52	129.40	3.275
ALMAmm14	290.91	14.51	40.68	10.44
ALMAmm32	290.92	14.52	69.29	8.458
e1mm1	290.93	14.51	61.88	15.10
ALMAmm31	290.92	14.52	103.13	9.828
ALMAmm33	290.92	14.52	123.62	8.361
ALMAmm35	290.92	14.52	127.47	8.546
d2	290.92	14.52	97.38	12.22
e2nw	290.93	14.51	43.90	29.86
ALMAmm24	290.92	14.52	127.47	14.059
e2w	290.93	14.51	2.73	1264.8
e8mm1	290.93	14.51	75.20	50.00
e2e	290.93315	14.51	47.31	87.14
e2e_peak	290.93	14.51	47.31	87.14
north	290.92	14.52	130.20	36.14

REFERENCES

[1]Adam Ginsburg *Thermal Feedback in...*

Friesen et al. 2017 - http://adsabs.harvard.edu/abs/2017ApJ...843...63F
Ginsburg et al. 2017 - https://arxiv.org/abs/1704.01434
Ginsburg 2018 - https://arxiv.org/abs/1702.06627v1